Available online at www.sciencedirect.com
SCIENCE DIRECT®
Journal of Organometallic Chemistry 671 (2003) 137–144
Journal of Organometallic Chemistry
www.elsevier.com/locate/jorganchem

Formation of an allylic cluster in the reactions of $[Ru_3(CO)_{12}]$ with diethylamino-propyne and trimethylsilyl propargyl alcohol. Crystal structure of $[(\mu\text{-H})Ru_3(CO)_9(\mu_3\text{-}\eta^3\text{-}C_3H_3)]$

Giuliana Gervasio [a,*], Domenica Marabello [a], Philip J. King [b], Enrico Sappa [c], Andrea Secco [c]

[a] Dipartimento di Chimica IFM, Università di Torino, Via Pietro Giuria 7, I-10125 Torino, Italy
[b] Department of Chemistry, University of Hull, Cottingham Road, Hull HU6 7RX, UK
[c] Dipartimento di Scienze e Tecnologie Avanzate, Università del Piemonte Orientale, Spalto Marengo 33, I-15100 Alessandria, Italy

Received 5 December 2002; received in revised form 3 February 2003; accepted 6 February 2003

Abstract

The title complex $(\mu\text{-H})Ru_3(CO)_9(\mu_3\text{-}\eta^3\text{-}C_3H_3)$ has been obtained following two different reaction pathways: one is the deamination of diethylaminopropyne, $HC{\equiv}CCH_2NEt_2$, in the presence of $Ru_3(CO)_{12}$ under thermal conditions. The other is the reaction of trimethylsilylpropargyl alcohol, $(HO)H_2CC{\equiv}C(SiMe_3)$ (TSPA), with $Ru_3(CO)_{12}$. The complex is obtained both under thermal conditions and in the reaction of the carbonyl with TSPA in CH_3OH/KOH (followed by acidification). Other reaction products, deriving from the loss of Me_3Si and of HCHO fragments from TSPA, have also been characterized. Complex $(\mu\text{-H})Ru_3(CO)_9(\mu_3\text{-}\eta^3\text{-}C_3H_3)$ has been spectroscopically characterized and its crystal structure was determined by an X-ray analysis. An isosceles triangle of Ru atoms with an edge bridged by an H atom, is coordinated by an allylic moiety σ-bonded to two Ru atoms and π-interacting with the third Ru atom.

Keywords: Allylic clusters; Diethylaminopropyne; Trimethylsilylpropargyl alcohol

1. Introduction

We are currently synthesizing inorganic–organometallic materials by including functionalized alkynes (alkynols, alkyne-diols, amino-alkynes) [1] into SiO_2 networks obtained through sol–gel procedures [2] and then reacting these solids with $Ru_3(CO)_{12}$. For a better characterization of these materials, we decided to synthesize, also, *models* of the alkyne cluster interactions [3]. We chose to perform these reactions both under thermal conditions and in KOH/CH_3OH solutions, that is in conditions closer to those presumably occurring on silica surfaces, where formation of cluster anions is likely to occur [4].

When reacting $Ru_3(CO)_{12}$ with diethylaminopropyne (DAP) in cyclohexane solution we obtained the allenylic derivative $(\mu\text{-H})Ru_3(CO)_9(H_2C{=}CC{=}NEt_2)$ (**1**) [5] and the title complex $(\mu\text{-H})Ru_3(CO)_9(\mu_3\text{-}\eta^3\text{-}C_3H_3)$ (**2**). The reaction of trimethylsilylpropargyl alcohol (TSPA) in benzene gave low yields of **2** which is the main product of the reaction of $Ru_3(CO)_{12}$ and TSPA in KOH/CH_3OH solution.

The molecule of **2**, determined by means of an X-ray analysis, contains an *unsubstituted* CHCHCH allylic group. Its structural features are compared with those of other *substituted* triruthenium allylic derivatives.

2. Experimental

2.1. General details, materials, analysis of the products

$Ru_3(CO)_{12}$ (Strem Chemicals) and the alkynes were commercial products (DAP from Aldrich, TSPA from Lancaster Synthesis) and were used as supplied. Solvents

* Corresponding author. Tel.: +39-011-6707504; fax: +39-011-6707855.
E-mail address: giuliana.gervasio@unito.it (G. Gervasio).

0022-328X/03/$ - see front matter © 2003 Elsevier Science B.V. All rights reserved.
doi:10.1016/S0022-328X(03)00094-9

(cyclohexane, heptane and benzene) were dehydrated over sodium. The reactions were performed under a dry nitrogen atmosphere in conventional three necked flasks equipped with gas inlet, cooler, mercury check valve and magnetic stirring.

The reaction mixtures (from the thermal reactions) were filtered under N_2, brought to small volume and separated on TLC plates (Merck Kieselgel P.F., eluent mixtures of hexane and diethyl ether in variable v/v ratios depending on the reaction mixtures). The KOH/CH_3OH solutions, after acidification, were extracted with heptane and the hydrocarbon solutions brought to small volume and chromatographed on TLC plates. Elemental analyses were performed in the Microanalytical Laboratory of the School of Chemistry, University of Bristol. The IR spectra were obtained on a Bruker Vector 22 (KBr cells, 0.5-mm path length) and on a Perkin-Elmer 1710 Fourier Transform spectrophotometer (CaF_2 cells, 1-mm path length). The ^{1}H- and ^{13}C-NMR spectra were obtained both with JEOL JNM 270/89, GX 270 and GX 400 spectrometers. The mass spectra (EI) were obtained with a Finnigan-Mat TSQ-700 mass spectrometer (servizio di Spettrometria di massa, Dipartimento di Scienza e Tecnologia del Farmaco, Università di Torino) The FAB mass spectra were obtained using a Fison Autospec instrument (University of Bristol).

2.2. Reaction of $Ru_3(CO)_{12}$ with DAP in cyclohexane

A cyclohexane solution (100 cm^3) of [$Ru_3(CO)_{12}$] (1.00 g; 3.52 mmol) and DAP (0.21 cm^3; 1.60 mmol) was heated at reflux point for 1 h, over which time a color change from orange to red was observed. Removal of solvent, under reduced pressure, and chromatography on alumina afforded the following bands: (i) yellow, eluted with hexane, which afforded yellow complex **1** (35% yield); (ii) yellow, eluted with hexane–dichloromethane (4:1), which yielded yellow complex **2** (20% yield).

2.3. Complex *1*

Found: C, 29.18; H, 2.01. Calc: C, 28.83; H, 1.97. IR (ν_{CO}) in hexane: 2083 vs, 2053 vs, 2033 vs, 2008 vs, 1998 vs(sh), 1985 vs, 1958 s, cm^{-1}. ^{1}H-NMR (CD_2Cl_2): δ 4.15 (m, 2H), 3.65 (m, 2H), 2.31 (s, 1H), 1.94 (s, 1H), 1.32 (m, 3H), 1.24 (m, 3H), −18.42 (d, 1H). ^{13}C-NMR (CD_2Cl_2): 224.2 (μ-*C*=N), 203.2–192.0 (all COs), 138.4 (μ-*C*=CH_2), 51.3 (N–*C*H_2), 45.3 (N–*C*H_2), 23.79 (C=*C*H_2), 12.8 (CH_3), 12.4 (CH_3) ppm. FAB mass spectrum, $m/z = 668$ [M$^+$] plus signals for successive loss of 8 carbonyls.

2.4. Complex *2*

Found: C, 24.31; H, 0.71. Calc: C, 24.11; H; 0.66. IR (ν_{CO}) in heptane: 2098 m, 2070 vs(sh), 2061 vs, 2046 vs, 2030 vs, 2011 s, 1990 m, cm^{-1}. ^{1}H-NMR (CD_2Cl_2): δ 8.58 (d, $J = 6.6$ Hz, 2 × μ-CH), 7.27(dt, $J = 6.6$, 2.1 Hz, CH), −20.78 (d, $J = 2.1$ Hz, μ-H). ^{13}C-NMR (CD_2Cl_2): 197.9–189.3 (all COs), 161.5 (2 × μ-CH), 116.9 (CH) ppm. FAB mass spectrum: $m/z = 598$ [P$^+$] [M$^+$] loss of 8 CO. Competitive fragmentation starting from 586 m/z [M$^+$–C] and loss of 8 CO. EI mass spectrum: [P$^+$] = 598 m/z, loss of 9 CO, intense peak at 342 m/z (Ru_3C_3).

2.5. Reaction of $Ru_3(CO)_{12}$ with TSPA in benzene

One gram of $Ru_3(CO)_{12}$ (ca. 3.2 mmol) was suspended in 100 cm^3 of benzene (previously purged with N_2) and 2 cm^3 of TSPA (ca. 15.6 mmol) was added. The solution was refluxed for 10 min, after which time the color changed from orange to red (clear solution). After TLC purification, two products were collected: yellow complex **2** (yield about 7%) and orange complex **3** (yield about 30%).

2.6. Complex *3*

Found: C, 25.0; H; 1.0. Calc: C, 24.8; H, 0.9. IR (CH_2Cl_2): 2097 m, 2072 vs, 2046 vs, 2026 s, 2014 s, 2010 s(sh) cm^{-1}. ^{1}H-NMR ($CDCl_3$, room temperature (r.t.)): δ 8.2 (d, 1H), 7.30 (dd, 1H), 4.7 (s, 2H), 2.60 (t, 1H), −20.1 (d, 1H). EI mass spectrum: $m/z = 628$ [P$^+$], release of 9 CO. Tentative identification $HRu_3(CO)_9$(HCCHC-CH_2OH)]. The ^{1}H-NMR of TSPA, for comparison is ($CDCl_3$, r.t.) δ 4.26 (dd, 2H), 2.38 (t, 1H), 1.54 (s, 9 H).

2.7. Reaction of $Ru_3(CO)_{12}$ with TSPA in CH_3OH/KOH solution

In a typical reaction 0.5 g (1.65 mmol) of $Ru_3(CO)_{12}$ were dissolved in 100 cm^3 of CH_3OH to which 10 pellets (about 1 g) of KOH had been added. The solution was warmed at 40 °C for 15 min until the color turned very dark brown. 1.5 cm^3 (ca. 12 mmol) of TSPA were then added and warming was continued for 30 min. After cooling, the solution was acidified with HCl (37%). The whitish precipitate (KCl) was filtered and the solution was extracted with heptane. The light yellow solution obtained was purified on TLC plates and gave yellow complex **2** (about 35% yield), trace amounts of a purple complex (unidentified) and a yellow complex (**4**) (about 10%).

2.8. Complex *4*

Found: C, 25.9; H, 1.4. Calc: C, 25.6; H, 1.5. IR: 2097 m, 2072 s, 2055 s, 2023 vs(b), 1990 m, cm^{-1}. ^{1}H-NMR:

δ 0.40 (s, 9H), −21.3 (s, 1H). ^{13}C-NMR: 1.6 s (Me), 74.0 s (C_β), 181.0 s (C_α), 188.3 s, 190.0 s, 193.1 s, 198.0 s, 199.9 s (int: 1,1,1,3,3) (CO). EI mass spectrum: $m/z =$ 656[P^+] (weak), release of 9 CO. Competitive fragmentation: release of fragments with 16 m/z (CH_4?). Tentative identification $HRu_3(CO)_9[C_2(SiMe_3)]$.

2.9. Crystallography

The data collection was made on a Siemens P4 diffractometer equipped with a Bruker APEX CCD detector using graphite-monochromated Mo–K_α radiation ($\lambda = 0.71073$ Å). The complex **2** (μ-H)$Ru_3(CO)_9(\mu_3$-η^3-$C_3H_3)$ crystallizes in triclinic $P\bar{1}$ space group, with $a = 6.8867(9)$ Å, $b = 8.677(1)$ Å, $c = 14.482(2)$ Å, $\alpha = 78.641(2)^\circ$, $\beta = 85.400(3)^\circ$, $\gamma = 73.633(3)^\circ$, $V = 813.7(2)$ Å^3, $M = 595.36$, $Z = 2$, $D_{calc} = 2.43$ g cm^{-3}, $\mu = 2.790$ mm^{-1}. The yellow crystal used was prismatic of dimensions $0.02 \times 0.12 \times 0.24$ mm. The θ range for measurement was 1.43–28.27°, 2775 reflections were measured at 293 K and 1949 were unique ($R_{int} = 0.033$). The absorption correction was made by numerical integration (min–max transmission factor 0.685–0.956). The refinement of 230 parameters was made using full-matrix least-squares on F^2. All non-hydrogen atoms were refined anisotropically. The hydrogen atoms were located on the last difference Fourier maps; the hydrogen atoms of the allylic moiety were refined with U_{iso}s set at 1.2 times U_{eq} of the corresponding C atom, while the hydridic H atom bridging the Ru–Ru bond was fully refined with satisfying results. The final parameters were: $R = \Sigma||F_o| - |F_c||/\Sigma|F_o| = 0.0277$ for 1498 'observed' reflections having $F_o^2 > 2\sigma(F_o^2)$, $wR = [\Sigma(wF_o^2 - F_c^2)^2/\Sigma w(F_o^2)^2]^{\frac{1}{2}} = 0.0555$, Goodness-of-fit = $[\Sigma w(F_o^2 - F_c^2)^2/(\text{no. of unique reflections} - \text{no. of parameters})]^{\frac{1}{2}} = 0.828$. Programs used were SHELXTL [6] for structure solution, refinement and molecular graphics, Bruker AXS SMART (diffractometer control), SAINT (integration), XPREP (absorption correction) [7].

3. Results and discussion

3.1. Spectroscopic identification of the complexes

The thermal reaction of DAP with $Ru_3(CO)_{12}$ yields (μ-H)$Ru_3(CO)_9(H_2C{=}CC{=}NEt_2)$ (**1**) as the main product and (μ-H)$Ru_3(CO)_9(\mu_3$-η^3-$C_3H_3)$ (**2**) in lesser amount. Complex **1** has been identified as an allenyl derivative, whose structure is similar to that of the amino-alkyne derivatives described by Deeming and coworkers [5].

The thermal reaction of TSPA with $Ru_3(CO)_{12}$ yields complex **3** as the main product and **2** in lesser amounts, confirming the hypothesis that, under thermal conditions, the formation of **2** is not the main process. For complex **3** we propose (on the basis of spectroscopic and mass spectral results) the allylic structure already found for the osmium complex [8] and shown in Scheme 1(below).

In contrast, the reaction of $Ru_3(CO)_{12}$ with TSPA in alkalyne methanolic solution, followed by acidification, yields **2** as the main product and complex **4** as the minor derivative. For complex **4** we propose the hydridic acetylidic structure shown in Scheme 1: the spectroscopic results found for **4** are well comparable, indeed, with those of (μ-H)$Os_3(CO)_9[C{\equiv}C(SiMe_3)]$ [9].

Complexes **1** and **3** could therefore represent intermediate stages of the fragmentation of DAP or of TSPA to give, as the final product, the allylic complex **2**. In contrast, complex **4** would be an end product.

3.2. Synthetic pathways leading to substituted allylic clusters and to the unsubstituted complex 2

A number of review articles dealing with propargyl activation [10] or with the reactivity of allenylic, allylic and related ligands both on mononuclear and on polynuclear metal centres [11] has appeared. Here we will discuss, in particular, the reaction pathways leading to the known family of substituted allyl derivatives. The unsubstituted complex **2** represents, indeed, the simplest example of this kind of structures; in addition it was obtained following reaction pathways not previously observed.

The first reported synthesis of an allylic hydridotriruthenium derivative was the oxidative addition of hex-3-yne on $Ru_3(CO)_{12}$ under thermal conditions: the allenyl (μ-H)$Ru_3(CO)_9$[MeCH=C=CEt] [12] was obtained, which isomerizes to (μ-H)$Ru_3(CO)_9$[MeCCH-CEt] [13]. Allenyl complexes can also be obtained upon thermal reactions of $Ru_3(CO)_{12}$ with pentenes [14], 1,3-butadiene or *cis*-2-butene [15].

These reactions could be compared with the dehydration and isomerization of diols (e.g. but-2-yn-1,4-diol, $HOCH_2CC{\equiv}CCH_2OH$) on $H_2Os_3(CO)_{10}$ to give, among others the osmium homologue of complex **3**, (μ-H)$Os_3(CO)_9$[CHCHC(CH_2OH)] [8].

Another important synthetic pathway is represented by the insertion of alkynes into M–X bonds. Examples are: (i) the insertion of acetylene (and loss of ethylene) into the methylidyne (μ-H)$_3Ru_3(CO)_9[\mu_3$-C(OMe)] to form (μ-H)$Ru_3(CO)_9$[CHCHC(OMe)] [16]. Coupling of alkyne and methylidyne (from alkyne metathesis) has also been observed on tetranuclear WOs_3 clusters [17] and on triosmium clusters [18]. (ii) Serendipity plays some role in the reaction of four molecules of HC≡CEt with $Fe_3(CO)_{12}$ to form, upon alkyne metathesis, $Fe_3(CO)_7[C_5H_2Et_3]$[EtCCHCH] [19]. Alkyne metathesis and formation of an allyl ligand also occurs on

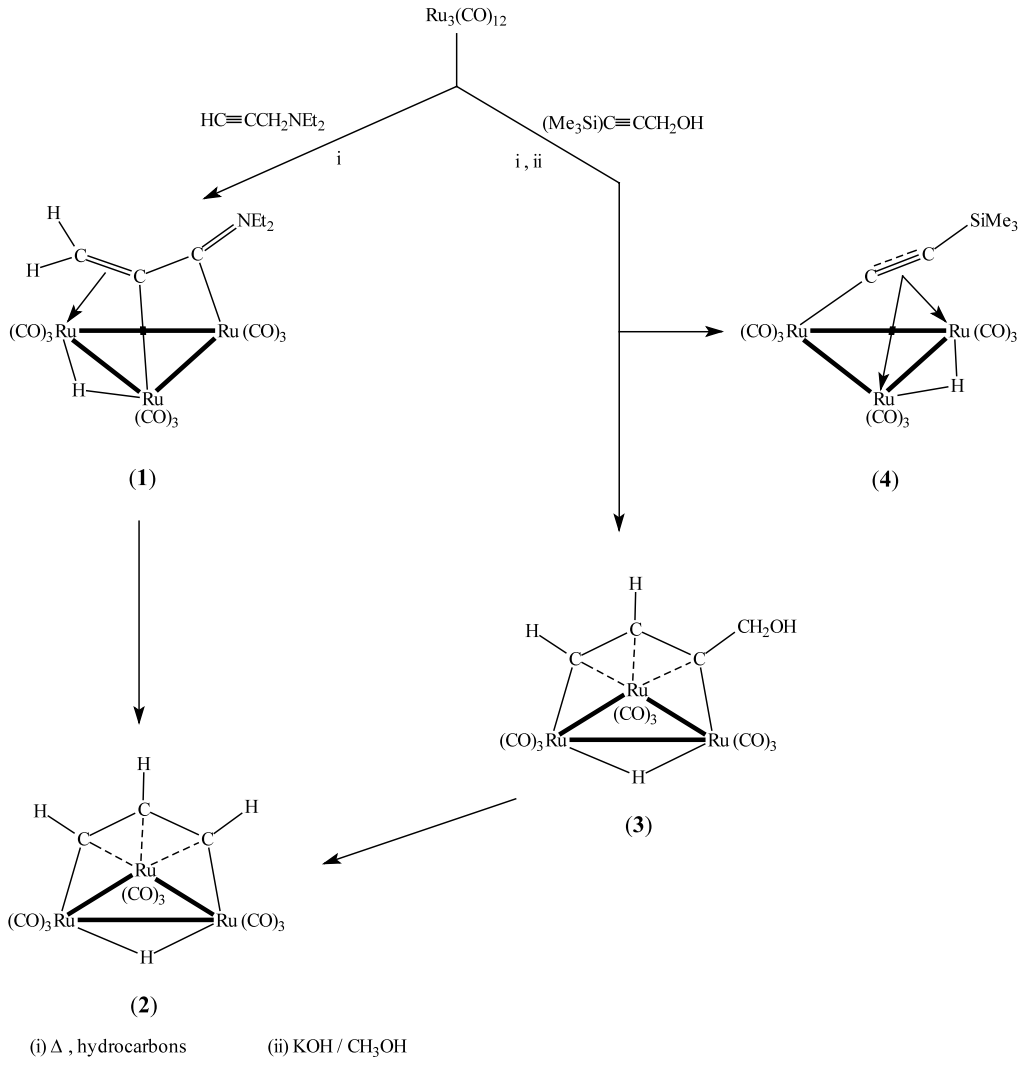

Scheme 1.

cyclopentadienyl (lightly ligated) triruthenium clusters with parallel alkynes [20].

Last, but not least, allylic structures were obtained upon coordination of amino-alkynes followed by isomerization on triruthenium clusters. Examples are the synthesis of (μ-H)$Ru_3(CO)_9$[CHCHC(NMe_2)] [5a] and of the allenylic (μ-H)$Ru_3(CO)_9$[MeC=CHC(=NMe_2)] 5b,5c,5d. Sometimes these reactions are promoted by Me_3NO [21].

The syntheses of complex **2**, reported in this paper, represent new approaches to the formation of unsubstituted allylic clusters. These reactions require the loss of fragments or of substituents of the amino-alkynes or of the TSPA ligand. In particular, DAP loses NEt_2 (presumably as Et_2NH and via allylic intermediates) and TSPA loses Me_3Si (presumably as Me_3SiX, X = H, Cl, OH depending on the reaction conditions) and oxygen and undergoes hydrogen shift. Loss of oxygen during reactions of alkynols with metal carbonyls has been previously observed [22]. Loss of trimethylsilyl groups has also been reported: treatment of $Os(CO)_9$(μ-CO)[$Me_3SiC_2C{\equiv}CSiMe_3$] with methanol gives $Os(CO)_9$(μ-CO)[$HC_2C{\equiv}CSiMe_3$] with loss of Me_3Si (as $HOSiMe_3$) [16].

Complexes **3** (loss of trimethylsilyl) is presumably an intermediate in the reaction leading to **2** as the final product. Complex **4** (loss of CH_2OH, presumably as HCHO and transfer of H to the metals) is, instead, a byproduct. Loss of oxygenated fragments or of water, and hydrogen shift, are common processes in the reactions of alkynols [4,23]. The proposed structures for complexes **1**–**4** and their relationships are shown in Scheme 1.

3.3. X-ray structure of complex 2

The structure of complex **2** is shown in Fig. 1 and relevant bond distances and angles are in Table 1.

The complex contains an isosceles triangle of ruthenium atoms, with the long Ru(1)–Ru(2) bond bridged

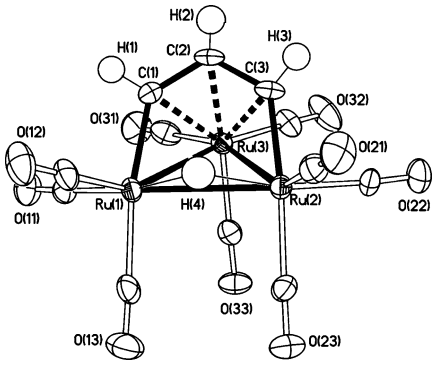

Fig. 1. ORTEP plot (30%) of the complex (μ_3-H)$Ru_3(CO)_9(\mu_3$-η^3-C_3H_3) (**2**).

by an hydridic atom. Three carbonyl ligands are bound to each ruthenium and those on Ru(1) and Ru(2) eclipse each other. The conformation of the $(CO)_3$ fragment is quite rigid and influenced by steric interaction with the allylic and hydride ligands. In fact the equatorial carbonyls CO(12) and CO(21) are tilted toward the allylic ligand and form an angle of 40° with the Ru_3 plane. The CO(11) and CO(22) groups are tilted in the opposite direction (Fig. 2).

The metal atom is the pivot around which the $(CO)_3$ group rotates. In fact on Ru(3) the equatorial carbonyls CO(31) and CO(32) are pushed away by the allylic ligand on the plane of the metal cluster and the CO(33) is folded toward Ru(1) and Ru(2). This situation cause also a distortion of the axial CO(33) which deviates from linearity (Ru(3)–C(33)–O(33) 170°). This deviation from linearity is not unusual; it can be observed also in other similar compounds [24]. The Ru(1,2)–C(13,23) distances *trans* to Ru(1)–C(1) and Ru(2)–C(3) are the longest ones, while the three Ru(3)–C_{CO} distances are equal. It is worthy of note that substitution of PPh_3 on substituted allylic derivatives occurs equatorially and *cis* to the hydride [15,21]. The hydride ligand bridges the Ru(1)–Ru(2) bond and is located between the two equatorial CO(12) and CO(21) groups; the Ru_2H plane forms an angle of 40° with the Ru_3 fragment (Fig. 2). The Ru–H(4) bond distances (1.81(7) Å av.) agree with the values found in complex (μ-H)$Ru_3(CO)_9[\mu_3$-η^2-C≡C–Bu^t] (1.792(5) Å av., neutron diffraction) [25], where however the hydride atom is below the Ru_3 plane on the opposite side with respect to the acetylenic ligand; these two opposite positions of the hydride atoms are consequence of the quite different geometry of the organic ligands; in fact in complex **2** the ligand is greatly shifted toward the Ru(3) atom, while in (μ-H)$Ru_3(CO)_9[\mu_3$-η^2-C≡C–Bu^t] the organic moiety is shifted toward Ru(1) and Ru(2). A search of CCDC shows that, in complexes containing (μ-H)$_n Ru_3$(n = 1,2,3) fragments, the hydride atom may lie below/above/on the cluster plane: the different situations greatly depend on the geometry of the organic ligand

Table 1
Selected bond lengths (Å) and angles (°) for (μ-H)$Ru_3(CO)_9(\mu_3$-η^3-C_3H_3) (**2**)

Ru(1)–C(12)	1.890(7)
Ru(1)–C(11)	1.903(9)
Ru(1)–C(13)	1.968(8)
Ru(1)–C(1)	2.051(7)
Ru(1)–Ru(3)	2.7796(7)
Ru(1)–Ru(2)	2.971(1)
Ru(1)–H(4)	1.85(7)
Ru(2)–C(21)	1.886(6)
Ru(2)–C(22)	1.900(9)
Ru(2)–C(23)	1.968(8)
Ru(2)–C(3)	2.037(7)
Ru(2)–Ru(3)	2.7893(8)
Ru(2)–H(4)	1.78(7)
Ru(3)–C(32)	1.911(8)
Ru(3)–C(33)	1.911(7)
Ru(3)–C(31)	1.915(10)
Ru(3)–C(1)	2.219(7)
Ru(3)–C(3)	2.232(7)
Ru(3)–C(2)	2.266(6)
C(1)–C(2)	1.394(12)
C(2)–C(3)	1.402(12)
H(1)···O(11)^{I}	2.53(7)
H(2)···O(31)^{II}	2.81(7)
H(4)···O(33)^{III}	2.84(7)
Ru(3)–Ru(1)–Ru(2)	57.92(2)
Ru(3)–Ru(2)–Ru(1)	57.60(2)
Ru(1)–Ru(3)–Ru(2)	64.48(2)
O(11)–C(11)–Ru(1)	177.4(7)
O(12)–C(12)–Ru(1)	176.5(8)
O(13)–C(13)–Ru(1)	177.0(7)
O(21)–C(21)–Ru(2)	176.5(6)
O(22)–C(22)–Ru(2)	175.7(8)
O(23)–C(23)–Ru(2)	178.2(7)
O(31)–C(31)–Ru(3)	178.2(9)
O(32)–C(32)–Ru(3)	178.1(6)
O(33)–C(33)–Ru(3)	170.5(5)
C(1)–C(2)–C(3)	119.9(8)
C(1)–H(1)···O(11)	154(4)
C(2)–H(2)···O(31)	152(5)
Ru(1)–H(4)···O(33)	120(3)
Ru(2)–H(4)···O(33)	128(3)

Roman numerals refer to the following positions: (I) $-x$, $1-y$, $1-z$; (II) $1-x$, $-y$, $1-z$; (III) $x-1$, y, z.

coordinated on the Ru_3 plane. In fact in highly symmetrical complexes as (μ-H)$_3Ru_3(\mu_3$-CR)$(CO)_9$ [26] the hydride atoms lie all below the cluster plane; when the organic ligand is asymmetrically bonded to the cluster as in (μ-H)$_2(\mu_3$-η^2-CHC(O)OCH_4)$(CO)_9$ [27] the less hindered hydride atom is on the cluster plane while the other is below the plane. The carbonyl groups adjacent to the hydride atoms are more or less pushed away by the insertion of the bridging H atom. In complex **2** the allylic fragment is bound to the three metal atoms through σ [Ru(1)–C(1) and Ru(2)–C(3)] and π-interactions [with Ru(3)]; the Ru_2C_3 moiety is planar (mean deviation from plane 0.035 Å) and forms an angle of 51° with the Ru_3 plane. The C(1)–C(2) and

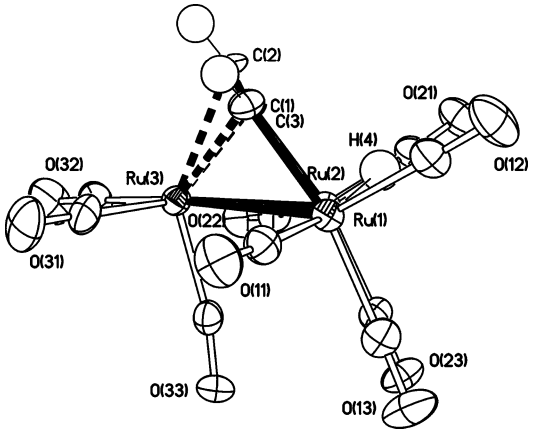

Fig. 2. View of the complex $(\mu_3\text{-H})Ru_3(CO)_9(\mu_3\text{-}\eta^3\text{-}C_3H_3)$ (**2**) with the geometry of $(CO)_3$ and hydride groups in evidence.

C(2)–C(3) bond distances, intermediate between a single and a double bond, and the C(1)–C(2)–C(3) angle of 120° agree with the allylic nature of the substituent (Table 1).

The synthesis and X-ray study of **2** offers the possibility of comparing the structural features of the unsubstituted complex with those of other ruthenium-containing substituted compounds of general formula $(\mu\text{-H})Ru_3(CO)_{9-n}L_n[RCCHCR']$ ($n = 1$–2, $L = PPh_3$, arsine). A search of CCDC gave twelve ruthenium structures with a similar arrangement. Selected bond distances and angles are collected in Table 2. Structures with $R > 0.10$ [13] and with atoms capping the Ru_3 cluster [28,29] were not reported in Table 2. The unbridged Ru–Ru and H-bridged Ru–Ru bonds, and two angles characterizing the geometry of allylic and hydride ligands are reported. In Table 2 we see that the allylic fragment has always the same orientation with respect to the Ru_3 plane, i.e. the dihedral angle between the Ru_3 plane and the plane of the allylic moiety is always nearly 50°. The angle formed by the Ru_2H plane with respect to the Ru_3 plane is in the wide range of 21–43°, with two unusual exceptions of H perpendicular to (VIBGUI) or in the Ru_3 plane (TAQTAG). This unusual behavior may be attributed to the big $C_{12}H_{19}$ ring (TAQTAG) and to the big $C_{12}H_{15}$ ring and arsine substituent (VIBGUI) respectively.

A comparison of other structural parameters shows that the bonding distances and angles of all the

Table 2
Structural parameters for allylic clusters

Formula	CSD code	Unbridged Ru–Ru (Å)	H bridged Ru–Ru (Å)	Angle A [a] (°)	Angle B [b] (°)	Ref.
$(\mu\text{-H})Ru_3(CO)_9(\mu_3\text{-}\eta^3\text{-HCCHCH})$		2.7796(7) 2.7893(8)	2.971(1)	51	40	this work
$(\mu\text{-H})Ru_3(CO)_8(PPh_3)(\mu_3\text{-}\eta^3\text{-HCCHCOH})$	CALDUO	2.783(1) 2.792(1)	2.986(1)	52	28	[28]
$(\mu\text{-H})Ru_3(CO)_9(\mu_3\text{-}\eta^3\text{-MeCCHCH})$	KUWPAT	2.784(1) 2.766(1)	2.941(1)	52	30	[15]
$(\mu\text{-H})Ru_3(CO)_8(PPh_3)(\mu_3\text{-}\eta^3\text{-MeCCHCH})$	KUWPEX	2.7905(3) 2.7946(3)	2.9690(3)	51	28	[15]
$(\mu\text{-H})Ru_3(CO)_7(PPh_3)_2(\mu_3\text{-}\eta^3\text{-MeCCHCH})$	KUWPIB	2.8096(5) 2.7865(5)	2.9895(5)	51	37	[15]
$(\mu\text{-H})Ru_3(CO)_9(\mu_3\text{-}\eta^3\text{-}C_{12}H_{17})$	PUKVUM	2.778(1) 2.786(1)	2.942(1)	51	41	[30]
$(\mu\text{-H})Ru_3(CO)_9(\mu_3\text{-}\eta^3\text{-MeCCMeCMe})$	SERBAS	2.777(2)	2.933(2)	52	39	[24]
$(\mu\text{-H})Ru_3(CO)_9(\mu_3\text{-}\eta^3\text{-MeCCMeCOMe})$	SERBEW	2.756(1) 2.774(1)	2.919(1)	53	30	[24]
$(\mu\text{-H})Ru_3(CO)_9(\mu_3\text{-}\eta^3\text{-MeCCMeCSEt})$	SERBIA	2.769(1) 2.795(1)	2.889(1)	51	21	[24]
$(\mu\text{-H})Ru_3(CO)_9(\mu_3\text{-}\eta^3\text{-}C_{12}H_{19})$	TAQTAG	2.797(2) 2.800(2)	2.956(2)	52	1	[31]
$(\mu\text{-H})Ru_3(CO)_9(\mu_3\text{-}\eta^3\text{-HCCPhCH})$	TORRIB	2.784(1) 2.805(1)	2.930(1)	51	43	[32]
$(\mu\text{-H})Ru_3(CO)_8(AsPh_2CH_2AsPh_2)(\mu_3\text{-}\eta^3\text{-}C_{12}H_{15})$	VIBGUI	2.775(1) 2.777(1)	2.982(1)	51	85	[33]
$(\mu\text{-H})Ru_3(CO)_7(PPh_3)_2(\mu_3\text{-}\eta^3\text{-MeCCMeCOMe})_2CH_2Cl_2$	WECNAT	2.787(2) 2.789(2)	2.966(2)	52	35	[21]

[a] Dihedral angle between the allylic moiety (Ru(1)Ru(2)C(1)C(2)C(3)) and the plane of Ru_3 cluster.
[b] Dihedral angle between the Ru(1)Ru(2)H(4) plane and the plane of Ru_3 cluster.

complexes follow the same trend. For all complexes of Table 2 the Ru(1)–C(1), Ru(2)–C(3) distances (range 2.05–2.10Å) and Ru(3)–C(1,2,3) distances (range 2.22–2.30 Å) are typical of Ru–C(σ) bonds and of Ru–C_3 π-interactions respectively.

The crystal packing analysis of complex **2**, shows that allylic hydrogen atoms are involved in intermolecular C–H···O bonds (Table 1). The intermolecular bond between the hydride H(4) atom and O(33) (Table 1) is by far the most important; it is in fact the first example of this kind of bond for a ruthenium cluster [34]. The hydrogen bonds give rise to double-layers of molecules nearly parallel to the *ab* plane of the unit cell. The layers face each other with carbonyl groups and are stacked along the *c* axis.

3.4. ^{1}H- and ^{13}C-NMR of substituted complexes and of 2

We have also compared the literature NMR data for complexes of the type (μ-H)$Ru_3(CO)_{9-n}L_n$(RCCHCR′) with those of complex **2**. The available examples are collected in Table 3.

It is worth noting that the ^{1}H chemical shifts of C(2)H and of the hydride vary considerably depending on the substituents on the allyl ligand and on the presence of PPh_3 groups, although in 6 of the 17 examples collected the C(2)H values fall in the range 6.0–7.5. In the few examples available of ^{13}C-NMR spectra the chemical shift of C(2) is in the narrow range 117–120, whereas those of the other allylic carbons vary depending on the substitution.

4. Conclusions

Cluster **2** has been synthesized for the first time following new—and somewhat unexpected—reaction pathways using as precursors the amino-alkyne DAP and the trimethylsylil alcohol TSPA. Cluster **2** is the (unsubstituted) parent of an allylic hydrido-triruthenium cluster family. Several (substituted) members showing this type of structure are known; their structures and NMR data have been discussed.

The reaction leading to cluster **2** require the loss of fragments from the amino-alkyne (DAP) or from the silyl-alkynol (TSPA) parent ligands. Loss of fragments from functionalized alkyne ligands, isomerization and hydrogen shift have already been reported separately [4,22,23]. The combination of two or more of these processes may, however, lead to new products which cannot be obtained—apparently—following the more straightforward procedures.

The results of the reactions performed under basic methanol conditions indicate that there is a close

Table 3
^{1}H- and ^{13}C-NMR chemical shifts for allylic clusters (μ-H)$Ru_3(CO)_{9-n}L_n$(R1CCHCR3)

R1	R3	^{1}H (C2)	Hydride	^{13}C (C1)	^{13}C (C2)	^{13}C (C3)	Ref.
H	H	7.27 dt	−20.78 d	160.2	117.0	162.0	this work
H	Me	6.96 dd	−20.41 d	159.45	117.53	190.42	[15]
H	Me [a]	6.93 dd	−19.70 dd	158.42	118.01	194.96	[15]
H	Me [b]	–	−18.5 b	–	119.26	195.62	[15]
Me	Me	3.32 d	−20.1 d	–	–	–	[14]
Me	Et	3.36 d	−20.2 d	–	119.8	–	[13]
MeO	OEt [c]	5.90 dd	−18.52 ddd	–	–	–	[21]
MeO	OEt [d]	3.47 q	−17.60 td	–	–	–	[21]
MeO	OEt [e]	6.12 dd	−17.20 br t	–	–	–	[21]
Me	NMe_2	6.00 d	−17.58 d	–	–	–	[5b,5c]
Me	NMe_2 [f]	5.43 d	−18.00 dd				[5b]
Me	NMe_2 [g]	5.86 d	−17.67 dd				[5b]
Me	NMe_2 [h]	5.90 d	−17.97				[5b]
H	NMe_2	6.03 dd	−18.50 d	–	–	–	[5a]
Me	NEt_2 [i]	4.20 dq	−17.71 dd	–	–	–	[21]
Me	NEt_2 [i]	3.98 dq	−17.23 dd	–	–	–	[21]
Me	NEt_2 [j]	4.20 dq	−16.40 td		–	–	[21]

[a] L = PPh_3, $n = 1$.
[b] L = PPh_3, $n = 2$.
[c] L = PPh_3, $n = 1$.
[d] L = PPh_3, $n = 2$.
[e] L = PPh_3, $n = 3$.
[f] L = $P(OPh)_3$, $n = 1$.
[g] L = PPh_3, $n = 1$.
[h] L = PPr^i_3, $n = 1$.
[i] L = PPh_3, $n = 1$, two isomers (phosphine close to R1 or R3).
[j] L = PPh_3, $n = 2$.

interconnection with the behavior of ligands and clusters in organometallic surface reactions [35] and that a variety of new results is still obtainable from alkyne cluster chemistry.

Acknowledgements

Financial support to this work has been obtained from MIUR (Rome) and Università del Piemonte Orientale, under the Cofin 2000 programme.

References

[1] We have chosen the alkynols and alkynediols because of the possibility of involving the OH functionalities into the hydrolysis–gelation processes of tetraethoxysilane. The amino-alkynes were chosen because their nitrogen-based substituents could catalyze the sol–gel processes acting as the ammonium-based catalysts currently used.
[2] (a) R.J.P. Corriu, D. Leclerq, Angew. Chem. Int. Ed. 35 (1996) 1420;
(b) U. Schubert, J. Chem. Soc. Dalton Trans. (1996) 3343.
[3] (a) G. Predieri, A. Tiripicchio, M. Tiripicchio Camellini, M. Costa, E. Sappa, Organometallics 9 (1990) 1729;
(b) E. Boroni, M. Costa, G. Predieri, E. Sappa, A. Tiripicchio, J. Chem. Soc. Dalton Trans. 2 (1992) 2585;
(c) G. Predieri, A. Tiripicchio, M. Tiripicchio Camellini, M. Costa, E. Sappa, J. Organomet. Chem. 423 (1992) 129.
[4] S. Deabate, P.J. King, E. Sappa, in: P. Braunstein, L.A. Oro, P.R. Raithby (Eds.), Metal Clusters in Chemistry, vol. 2 (Chapter 8), Wiley-VCH, Weinheim, 1999, p. 796.
[5] (a) S. Aime, D. Osella, A.J. Arce, A.J. Deeming, M.B. Hursthouse, A.M.R. Galas, J. Chem. Soc. Dalton Trans. (1984) 1981;
(b) S. Aime, G. Jannon, D. Osella, A.J. Deeming, J. Organomet. Chem. 214 (1981) C15;
(c) S. Aime, G. Jannon, D. Osella, A.J. Arce, A.J. Deeming, J. Chem. Soc. Dalton Trans. (1984) 1987;
(d) S. Aime, D. Osella, A.J. Deeming, A.J. Arce, M.B. Hurshouse, H.M. Dawes, J. Chem. Soc. Dalton Trans. (1986) 1459 (Allenylic complexes such as $HRu_3(CO)_9[H_2C{=}CC{=}NMe_2]$ and $HRu_3(CO)_9[MeC{=}CC(H){=}NMe_2]$ were already reported).
[6] G.M. Sheldrick, SHELXTL, Version 5.1, Bruker AXS Inc., Madison, WI, 1997.
[7] SMART, SAINT, XPREP software for CCD diffractometers, Bruker AXS Inc., Madison, WI.
[8] S. Aime, A. Tiripicchio, M. Tiripicchio Camellini, A.J. Deeming, Inorg. Chem. 20 (1981) 2027.
[9] B.F.G. Johnson, J. Lewis, M. Monari, D. Braga, F. Grepioni, J. Organomet. Chem. 377 (1989) C1.
[10] A. Wojcicki, C.E. Schuchart, Coord. Chem. Rev. 105 (1990) 35.
[11] (a) M.I. Bruce, Chem. Rev. 91 (1991) 197;
(b) S. Doherty, J.F. Corrigan, A.J. Carty, E. Sappa, Adv. Organomet. Chem. 37 (1995) 39;
(c) M. Gruselle, H. Amouri, Chem. Rev. 96 (1996) 7.
[12] G. Gervasio, D. Osella, M. Valle, Inorg. Chem. 15 (1976) 1221.
[13] M. Evans, M. Hursthouse, E.W. Randall, E. Rosenberg, L. Milone, M. Valle, J. Chem. Soc. Chem. Commun. (1972) 545.
[14] M. Castiglioni, L. Milone, D. Osella, G.A. Vaglio, M. Valle, Inorg. Chem. 15 (1976) 394.
[15] K.M. Rao, R.J. Angelici, V.G. Young, Jr., Inorg. Chim. Acta 198-200 (1992) 211.
[16] L.P. Clarke, J.E. Davies, P.R. Raithby, M.A. Rennie, G.P. Shields, E. Sparr, J. Organomet. Chem. 609 (2000) 169.
[17] M.-T. Kuo, D.-K. Hwang, C.-S. Liu, Y. Chi, S.-M. Peng, G.-H. Lee, Organometallics 13 (1994) 2142.
[18] W.-Y. Wong, S. Chan, W.-T. Wong, J. Chem. Soc. Dalton Trans. (1995) 1497.
[19] E. Sappa, A. Tiripicchio, A.M. Manotti-Lanfredi, J. Chem. Soc. Dalton Trans. (1978) 552.
[20] S.A.R. Knox, J.Cluster Sci. 3 (1992) 385.
[21] M.R. Churchill, C.H. Lake, R.A. Lashewycz-Rubycz, H. Yao, R.D. McCargar, J.B. Keister, J. Organomet. Chem. 452 (1993) 151.
[22] G. Gervasio, E. Sappa, Organometallics 12 (1993) 1458.
[23] (a) G. Gervasio, R. Gobetto, P.J. King, D. Marabello, E. Sappa, Polyhedron 17 (1998) 2937;
(b) J.P.H. Charmant, G. Davies, P.J. King, J. Wigginton, E. Sappa, Organometallics 19 (2000) 2330;
(c) J.P.H. Charmant, P. Crawford, P.J. King, R. Quesada-Pato, E. Sappa, J. Chem. Soc. Dalton Trans. (2000) 4390;
(d) J.P.H. Charmant, P.J. King, R. Quesada-Pato, E. Sappa, C. Schaefer, J. Chem. Soc. Dalton Trans. (2001) 46.
[24] M.R. Churchill, L.A. Buttrey, J.B. Keister, J.W. Ziller, T.S. Janik, W.S. Striejewske, Organometallics 9 (1990) 766.
[25] M. Catti, G. Gervasio, S.A. Mason, J. Chem. Soc., Dalton Trans. (1977) 2260.
[26] N.J. Zhu, C. Lecomte, P. Coppens, J.B. Keister, Acta Cryst. B38 (1982) 1286
See for example complex $(\mu\text{-}H)_3Ru_3(CO)_9(\mu_3\text{-}CCl)$
[27] M.R. Churchill, T.S. Janik, T.P. Duggan, J.B. Keister, Organometallics 6 (1987) 799.
[28] M.I. Bruce, N.N. Zaitseva, B.W. Skelton, A.H. White, J. Chem. Soc. Dalton Trans. (1999) 2777.
[29] D. Ellis, L.J. Farrugia, J. Cluster Sci. 12 (2001) 243.
[30] M.I. Bruce, H.K. Fun, B.K. Nicholson, O. bin Shawkataly, R.A. Thomson, J. Chem. Soc. Dalton Trans. (1998) 751.
[31] K.O. Kallinen, M. Ahlgrén, T.T. Pakkanen, T.A. Pakkanen, J. Organomet. Chem. 510 (1996) 37.
[32] A.J. Blake, P.J. Dyson, P.E. Gaede, B.F.G. Johnson, S. Parsons, Organometallics 15 (1996) 4100.
[33] H.K. Fun, O. bin Shawkataly, S.G. Teoh, Acta Cryst. C46 (1990) 2329.
[34] D. Braga, F. Grepioni, E. Tedesco, K. Biradha, G.R. Desiraju, Organometallics 15 (1996) 2692.
[35] P.J. King, E. Sappa, C. Sciacca, Inorg. Chim. Acta 334 (2002) 131.